J Mater Sci: Mater Electron (2017) 28:3067–3074
DOI 10.1007/s10854-016-5894-2

Au NPs/ITO prepared by dopamine reduction and its application in glucose sensing

Jiali Li[1] · Luting Yan[1] · Huili Wang[1] · Haiwei Wang[1] · Xiao Chen[1] · Lei Wang[1] · Meng Wu[1]

Received: 22 July 2016 / Accepted: 12 October 2016 / Published online: 15 October 2016

Abstract Gold nanoparticles (NPs) were deposited directly on an indium tin oxide (ITO) substrate using the successive ionic layer adsorption and reaction (SILAR) method by chemically reducing precursor metal salts with dopamine aqueous solution. The Au NPs decorated on the ITO substrate were approximately spherical, with an average particle size of about 40 nm, which varied in accordance with different SILAR cycles, reactant concentrations, and intermediate media. Strong surface plasma resonance characteristics were confirmed by the surface-enhanced Raman scattering and absorption spectra of the Au NPs. Through this simple method, glucose sensors based on this kind of Au NPs/ITO exhibited a sensitivity of 524 μA mM^{-1} cm^{-2}, which is higher than any other similar study.

1 Introduction

Transparent conducting oxide (TCO) films are widely employed in optoelectronic devices, such as flat panel displays, solar cells, touch panels, light-emitting diodes, and smart windows. Indium tin oxide (ITO), as the most commonly used TCO material, has been used as electrode and applied in the study of electrochemical active substances because of its high conductivity, wide potential window, and high transparency [1, 2]. Meanwhile, gold nanoparticles (NPs), given their unique optoelectronic characteristics, have been used widely in many applications, such as catalysts, sensors, organic photovoltaics, and drug delivery systems [3]. By combining suitable properties, Au-NP-modified ITO electrodes can be adopted in biological detection, catalysis, and sensor operation as reported in several studies. Au NPs were electrodeposited on ITO glass surfaces and employed for the electrochemical detection of heavy metal ions [4]. The enhanced electrochemiluminescence of peroxydisulfate was observed on the Au NPs electrodeposited on an ITO electrode, which was used to detect glucose with high sensitivity and considerable selectivity. Au NPs were employed to act as tiny conduction centers with large apparent surface areas that facilitate electron transfer and strongly immobilize the enzymes by amine groups and cysteine residues. As such, the NPs greatly enhance the electrochemiluminescence intensity and improve the sensitivity of the resultant biosensor [5]. ITO electrodes modified with Au NPs and functionalized with a self-assembled film of L-cysteine have been used for sensing ascorbic acid. Cyclic voltammetric study revealed that the electrode exhibited excellent electrocatalytic activity toward the oxidation of ascorbic acid [6]. Au-NP-modified ITO substrate has also been used for excited surface plasmon resonance (SPR). A sputtering-deposited Au NPs/ITO anode was employed in green-emitting polymer light-emitting diode (PLED), in which the electroluminescence intensity increased nearly by 2.7 fold, compared with that of the standard PLED with a bare ITO substrate [7].

The methods used for obtaining Au-NP-attached ITO substrate involve spin coating pre-synthesized Au NP suspensions on the substrate, electrochemical deposition, and sputtering deposition of Au NPs on the substrate [8, 9]. However, these processes are time consuming and complicated. In our previous work, the direct attachment and growth of Au and Ag NPs on ITO surfaces was attempted

✉ Luting Yan
ltyan@bjtu.edu.cn

[1] School of Science, Beijing Jiaotong University, Beijing 100044, People's Republic of China

using a simple and inexpensive successive ionic layer adsorption and reaction (SILAR) method by chemical reduction of the precursor metal salts with dopamine aqueous solution, and the Au -Ag NPs decorated ITO substrates were tried for polymer solar cell [10]. In this work, further studies focus on SILAR cycles, reactant concentrations, and intermediate media. The structure, morphology, and SPR characteristics were measured. Glucose sensors based on this kind of Au NPs/ITO showed the same sensitivity and stability as those of Au NPs/ITO obtained by electrodeposition or seed-mediated growth [11, 12]. However, the method presented in this paper is more simple and convenient.

2 Experimental

2.1 Materials and apparatus

ITO glass (1 mm thickness, resistance <10 Ω/sq) was purchased from Zhuhai Kaivo Optoelectronic Technology Co., Ltd. (ZhuHai, China). Dopamine hydrochloride (98 %) was purchased from Aladdin Industrial Corporation. Hydrogen tetrachloroaurate (III) trihydrate ($HAuCl_4 \cdot 3H_2O$, 99.9 %) was acquired from Sigma–Aldrich. Potassium hydrate, sodium hydrate, acetone, alcohol, and sulfuric acid were purchased from Beijing Chemical Works. D-(+)-Glucose was purchased from Sinopharm Chemical Reagent Co., Ltd. All the chemicals were used as received.

2.2 Preparation of Au-NP-decorated ITO substrate

ITO glass was boiled with a water-diluted detergent for 1 h. Then, the glass was washed with acetone, ethanol, and distilled water for 30 min successively in an ultrasonic bath. After drying in argon, Au/ITO was fabricated using the following methods.

The ITO substrate was immersed vertically into a dopamine solution, intermediate medium (distilled water or sodium hydroxide solution), and $HAuCl_4$ aqueous solution, each for 15 s. This procedure was repeated for different cycles. Finally, the ITO substrate was rinsed with deionized water and dried in argon.

2.3 Characterization

The surface morphologies of the Au NPs were observed by field-emission scanning electron microscopy (SEM; FEI NanoSEM-230). The metal NP structure was characterized through X-ray diffraction (XRD; PANalytical Xpert Materials Research diffractometer system) with a Cu Kα radiation source ($\lambda = 0.1541$ nm) at 45 kV and 40 mA. Transmission and reflection spectra were measured using a Perkin Elmer UV–Vis spectrometer (Lambda 1050). Electrochemical properties were then investigated on a CHI760E workstation.

2.4 Electrochemical catalysis of glucose

Cyclic voltammetry (CV) was employed to examine the electrochemical response of glucose to Au NPs/ITO. Au NPs/ITO was used as working electrode and subjected to potential cycling from −0.20 to 1.60 V against a calomel electrode at a scan rate of 100 mV/s in 0.5 M H_2SO_4 to calculate for the electrochemically active surface areas (EASAs). The oxidation of glucose on Au NPs/ITO was conducted using a platinized platinum as the counter electrode and a $Hg|Hg_2Cl_2|KCl$ (sat.) as the reference electrode in a 0.5 M potassium hydroxide solution containing glucose at a scan rate of 10 mV/s. The actual area of the Au NPs/ITO electrode immersed into the electrolyte was limited to 0.25 cm^2.

3 Results and discussion

3.1 Morphology and crystal structure of Au NPs

In the dopamine molecule, two hydroxyl groups at the ortho positions were the main reaction groups for the metal ion reduction. During this oxidation process, the dihydroxy molecules lost two electrons to form a quinone structure. Simultaneously, Au ions accepted electrons to form Au NPs. The quinone groups would adsorb onto the surface of Au NPs and partially rearrange and polymerize to form polydopamine. Polydopamine holds strong adhesive abilities, which were favorable for stabilizing Au NPs on the ITO substrate. The states of Au NPs at different SILAR cycles, reactant concentration, and intermediate media were then studied.

Morphology of Au NPs with different SILAR cycles. Figure 1 shows the SEM images of Au NPs attached on the ITO substrate prepared at different SILAR cycles. We found that the Au NPs were approximately spherical and exhibited a narrow particle size distribution. Most of the Au NPs showed good dispersion, with sizes less than 50 nm. The average particle size of the Au NPs fabricated after 10 SILAR cycles was 36 nm, which was based on the measurement of 94 Au NPs. Meanwhile, the attachment density of the Au NPs on the ITO substrate increased with the increase in the number of SILAR cycles.

Morphology of Au NPs with different $HAuCl_4$ precursor concentrations. Figure 2 shows that the $HAuCl_4$ precursor concentration influenced the particle size and size distribution of the Au NPs when the concentration of

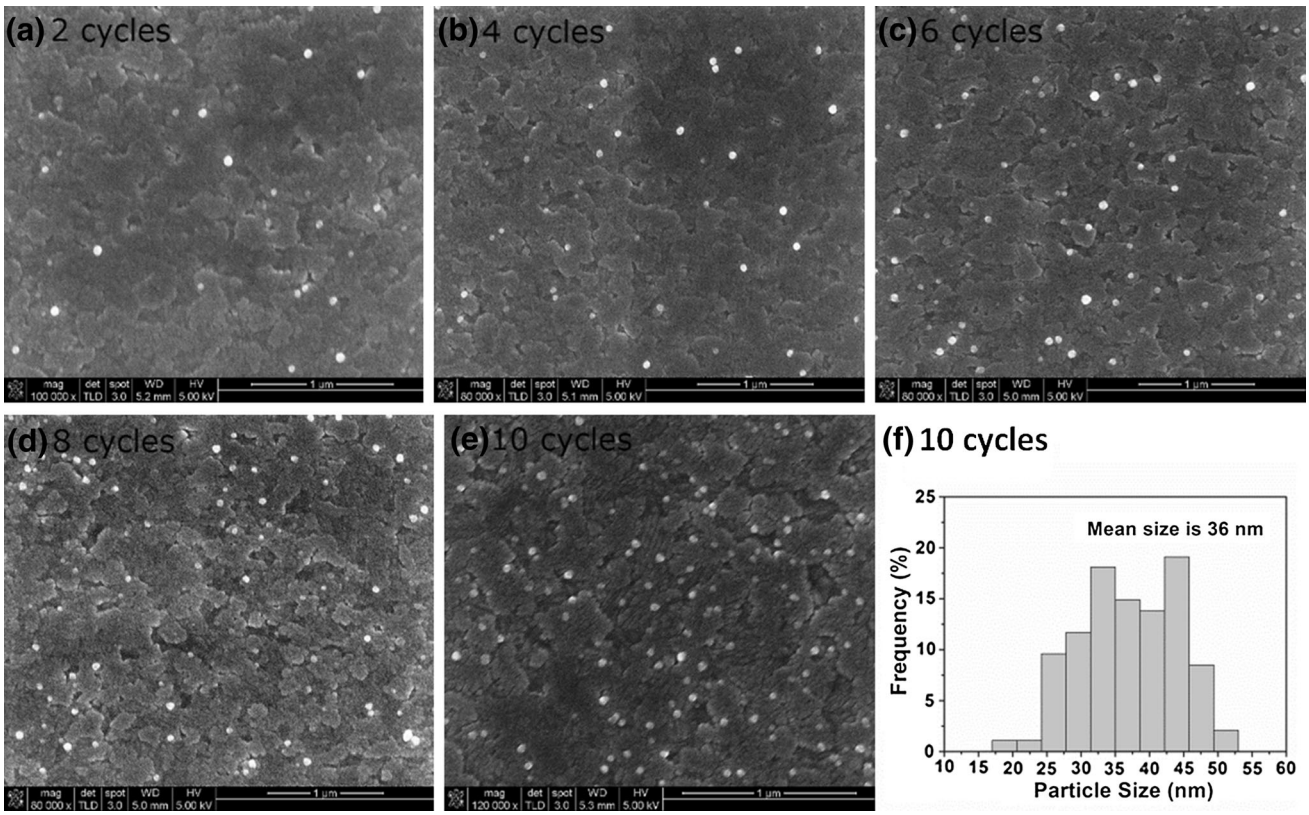

Fig. 1 SEM images of the Au NPs at different SILAR cycles (DA concentration = 0.24 mM; $HAuC_{l4}$ concentration = 0.3 mM) **a** 2 cycles; **b** 4 cycles; **c** 6 cycles; **d** 8 cycles; **e** 10 cycles and **f** particle size distribution of Au NPs fabricated with 10 SILAR cycles

dopamine remained unchanged at 0.24 mM. The Au NPs synthesized from 0.3 mM $HAuCl_4$ served as reference, and the size of Au NPs increased with the increase in starting $HAuCl_4$ concentration. The average sizes of the Au NPs generated from 0.7 to 1.4 mM $HAuCl_4$ were 62 and 73 nm, respectively. The size uniformity was also reduced. On the contrary, the attachment density of the Au NPs greatly decreased with the increase in the starting $HAuCl_4$ concentration. Under a lower starting $HAuCl_4$ concentration, the same phenomenon occurred, particularly, the size of the Au NPs increased and the attachment density slightly decreased. The two stages of the growth process that ensued during the Au NP formation were as follows: nucleation and growth of the primary nanoclusters, formation of secondary NPs with size selection, and relaxation process via the coalescence or aggregation of the primary nanoclusters. With a high concentration of $HAuCl_4$ precursor, more gold nanoclusters were generated as seeds. As a result, the Au NPs of smaller sizes are formed and attached on the ITO substrates. Further increase in the $HAuCl_4$ precursor cause generated a greater number of gold nanoclusters, and the process of formation of the secondary NPs became dominant and resulted in an increasing size and decreased attachment density.

Morphology of Au NPs with different intermediate medium. The intermediate medium influenced the morphology of the Au NPs mainly by adjusting the polymerization of dopamine. Dopamine can spontaneously polymerize in alkaline aqueous solution to form a thin adhesive layer of polydopamine on the surface of the ITO substrate. Polydopamine appeared as a stronger reducing agent than dopamine, and the adhesion of polydopamine was favorable for stabilizing Au NPs on the ITO substrate. In the strongly alkaline solution, polymerization accelerated and easily formed agglomerates, contrary to what we expected. Thus, at this point, we chose sodium hydroxide solution (pH 8) and distilled water as media intermediates for comparison. Figure 3 shows that the intermediate medium could also influence the particle size and size distribution of the Au NPs. Dopamine was appropriately polymerized in the sodium hydroxide solution (pH 8) and the reduction and adhesion were well combined. Therefore, the obtained Au NPs exhibited a narrower particle size distribution and higher attachment density compared with those fabricated in distilled water.

Crystal structure of the Au NPs. The phase structure of the obtained Au NPs were analyzed by XRD (Fig. 4). Four characteristic peaks ($2\theta = 38.08$, 44.42, 64.40, 77.84) corresponding to the (111), (200), (220), and (311) planes,

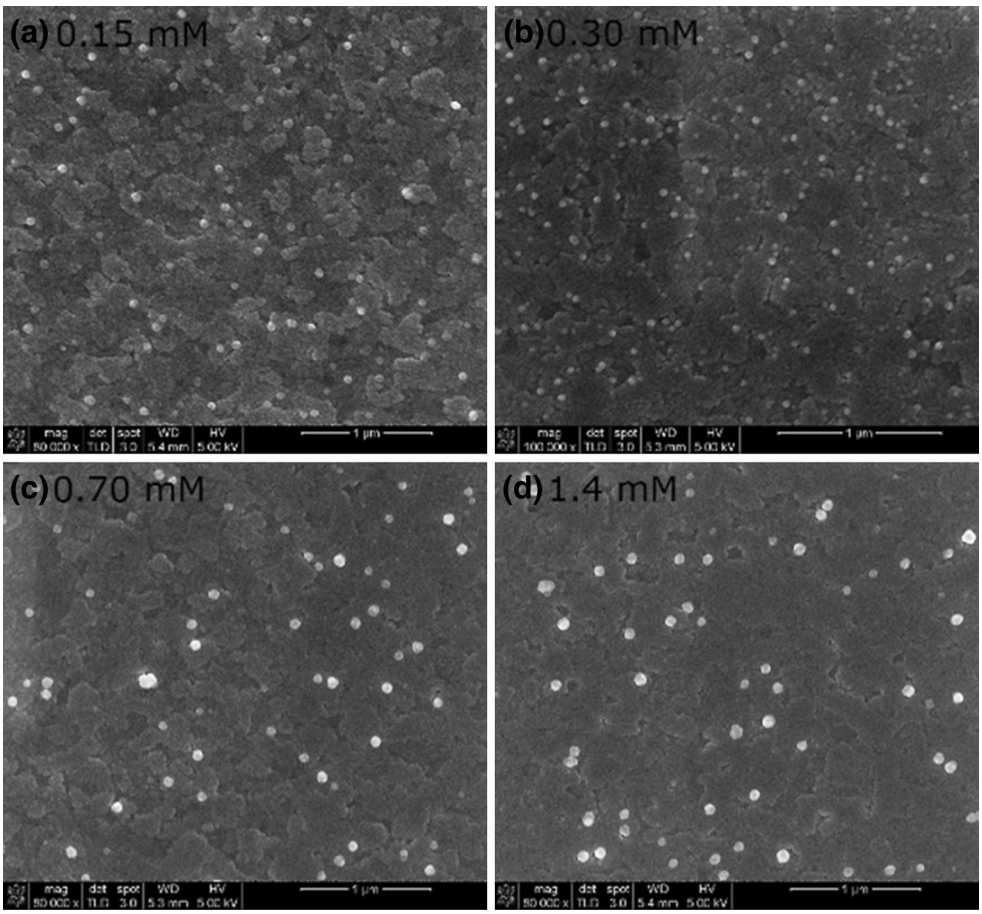

Fig. 2 SEM images of the Au NPs fabricated under 10 SILAR cycles at different $HAuCl_4$ concentrations as follows **a** 0.15, **b** 0.30, **c** 0.70, and **d** 1.4 mM

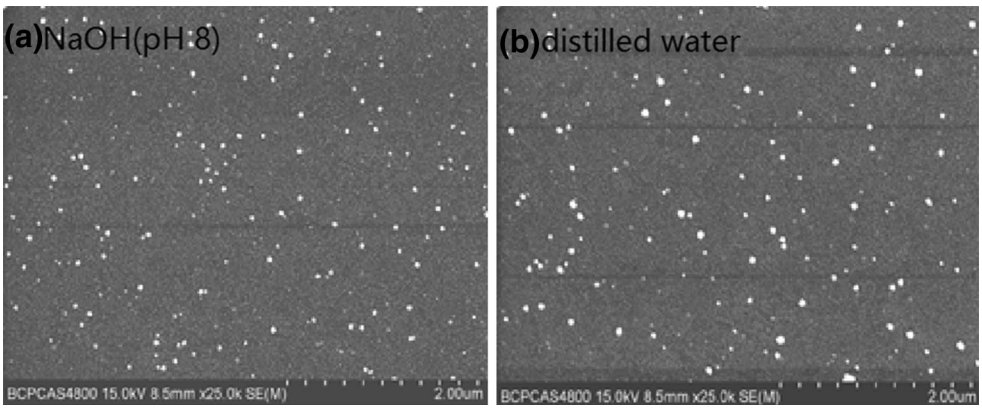

Fig. 3 SEM images of the Au NPs synthesized with two different intermediate media **a** sodium hydroxide solution (pH 8) and **b** distilled water

respectively, are clearly presented, indicating that the Au NPs were successfully produced.

3.2 SPR characteristics

SPR can provide a remarkably enhanced electromagnetic field around a metal surface. SPR is an enhancement model that explains the surface-enhanced Raman scattering (SERS) phenomenon. Meanwhile, SERS is a promising technique that can be used for ultra-sensitive chemical detection. A substantial enhancement of Raman scattering reaching 10^{14} can be achieved when molecules are adsorbed onto or placed near a noble metal surface. Hence, dopamine–quinone or polydopamine molecules adsorbed

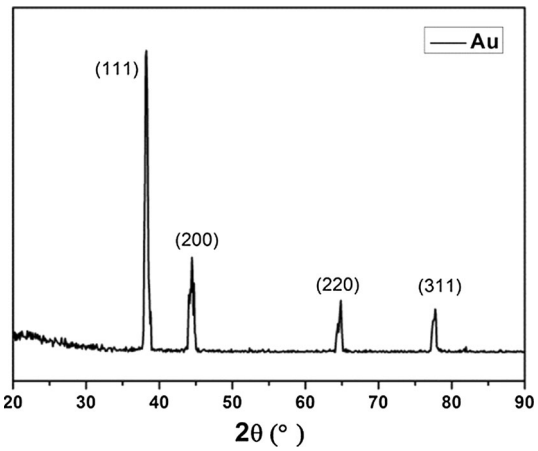

Fig. 4 XRD patterns of the Au NPs generated by dopamine reduction

on the surface of the Au NPs may be detected by SERS. In our study, the same SILAR process was employed on glass slides instead of ITO substrates, and the number of SILAR cycles were augmented to increase the amount of adhered metal NPs and enhance the SERS signal. Figure 5 reveals the SERS spectra of the Ag and Au NPs recorded under the 633 nm excitation wavelength. The characteristic Raman bands of dopamine–quinone at 1280, 1335, and 1450 cm^{-1} are presented. The bands at 1280 and 1335 cm^{-1} were assigned to the catechol C–O stretch [13, 14]. The relatively small peak at around 1450 cm^{-1} was assigned to the ring stretching vibration contributed mainly by the stretching of the carbon–carbon bond to which the oxygen was attached. Meanwhile, the band at 1567 cm^{-1} can be identified with the benzene modes υ_{8a} [15].

The optical properties of the Au attached to the ITO substrate are shown in Fig. 6. The transmission and reflection spectra of the Au NPs attached to the ITO substrate were first measured by a Perkin Elmer UV–vis spectrometer. Absorption was then calculated by

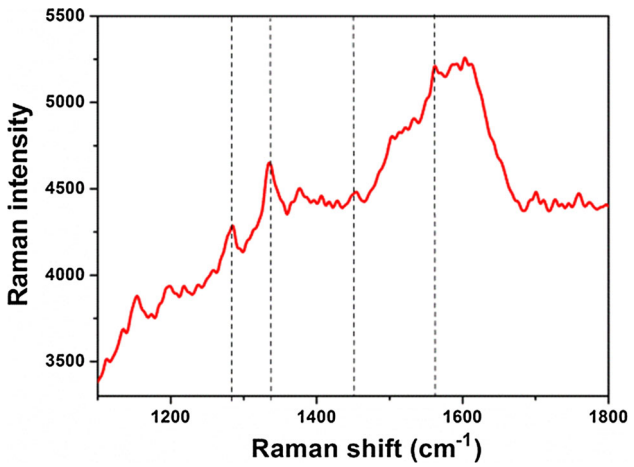

Fig. 5 SERS spectra of the Au NPs decorated on glass slides

$100 - R - T$, followed by deducing the absorption of the ITO substrate. The absorption peak at around 615 nm was derived from the excitation of the SPR peak of the Au NPs. According to the Mie theory, the SPR mainly depends on the free electron density of metal NPs. The SERS spectra confirmed that a small amount of dopamine–quinone adsorbed onto the surface of the Au NP; hence, the amino group of dopamine may have attracted the free electrons of the Au NPs and reduced the electron density of the Au NPs. This occurrence may have led to the red shift of the SPR absorption peak. The absorption of dopamine on the surface of the metal NPs may have also generated a bridging effect and caused some aggregation of the Au NPs and, consequently, a red shift.

3.3 Electrocatalytic activity of Au NPs/ITO toward glucose oxidation

Glucose detection is highly important in medical diagnosis, the food industry, and glucose–oxygen fuel cells. Currently, glucose sensors based on the electrocatalytic oxidation of glucose have attracted considerable attention because of the sensor's quick response, easy operation, and high selectivity. CV was employed to examine the electrochemical response of glucose to the Au NPs/ITO, and the EASAs were first calculated. Figure 7a shows the CV curve of the Au NPs/ITO in 0.5 M H_2SO_4. The calculated EASA value was 0.02 cm^2, which is about 8 % of the actual area.

Figure 7b shows the CV curve of the Au NPs/ITO in a 0.5 M KOH solution at a scan rate of 10 mV/s. These CV curves were similar to those of previous reports [16]. The first oxidation peak at around −0.36 V can be attributed to the electrochemical adsorption of glucose that produces an adsorption intermediate, namely, gluconolactone. At this point, the electrode remained in a reducing environment, and the AuOH sites of the active species on the surface of Au NPs were limited [17, 18]. When a large amount of AuOH sites formed on the electrode surface at around −0.1 V, subsequent oxidation of gluconolactone occurred, which corresponds to the second oxidation peak. As the potential continued to move forward, gold oxide was formed at around 0.275 V. The third oxidation peak was considerably weak relative to the first two peaks. At 0.4 V, the current densities in the CV curves disappeared. In the negative phase, the amount of surface gold oxide decreased at 0.1 V. As a result, sufficient surface active sites were formed, which were beneficial to direct glucose oxidation. A sharp oxidation peak appeared during a negative sweep up to 0.01 V [19].

To test the detection range and sensitivity of the Au NPs/ITO sensor, CV curves with different glucose concentrations were measured. The four oxidation peak

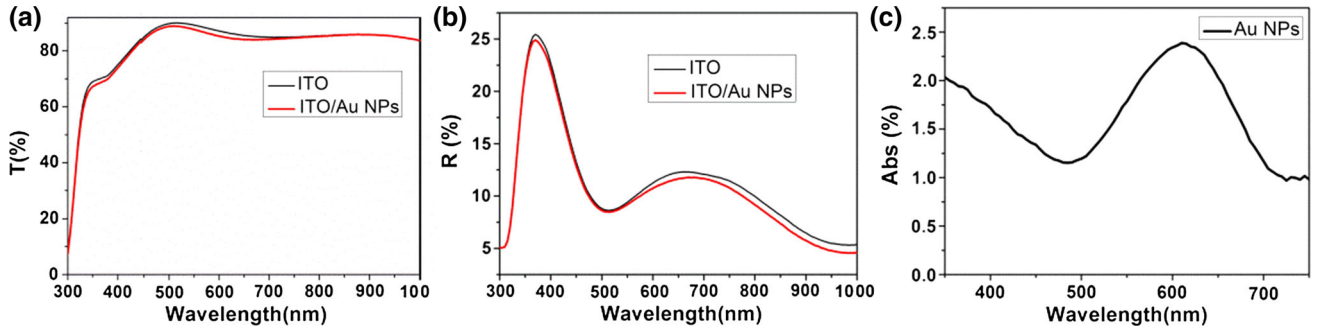

Fig. 6 Optical property of Au attached ITO substrate **a** transmission; **b** reflection; **c** absorption spectra of Au NPs

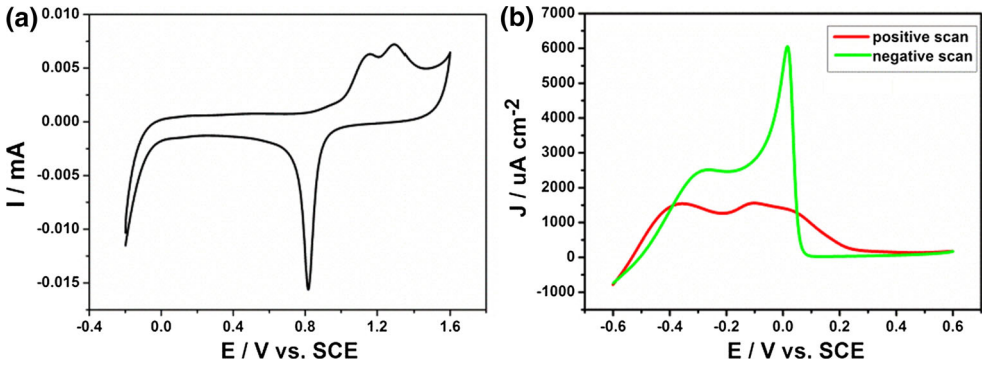

Fig. 7 **a** CV of the Au NPs/ITO in 0.5 M H_2SO_4 at a scan rate of 50 mV/s. **b** CV of the Au NPs/ITO in a 0.5 M KOH solution at a scan rate of 10 mV/s (10 mM glucose concentration)

intensities increased with the rising glucose concentration (Fig. 8a and b). Meanwhile, Fig. 8c and d show the correction curve of the current intensity of the four peaks with the change in glucose concentration. Peak B displays the best linear relationship and the maximum slope, which reflects high sensitivity. The detection sensitivity of peak B was 524 μA mM^{-1} cm^{-2}, and the linear correlation coefficient was 0.983. These values were similar or even higher

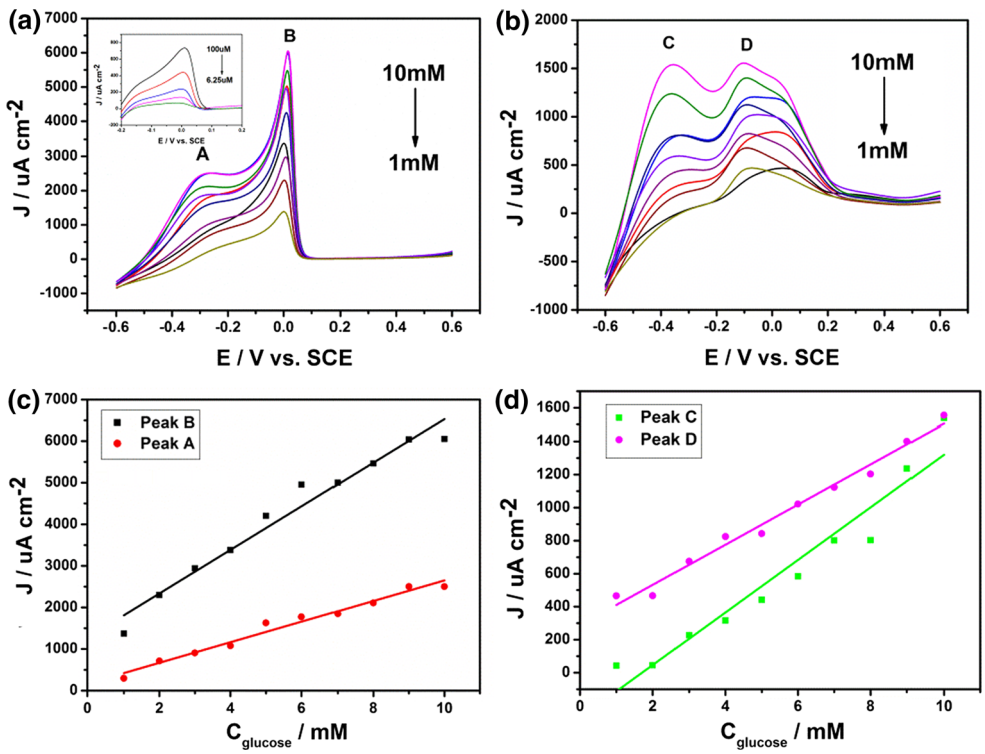

Fig. 8 CV *curves* of the Au NPs/ITO electrode in 0.5 M KOH with different glucose concentrations. **a** Negative scan; the inset corresponds to the glucose concentrations varying from 100 to 6.25 μM by half for every concentration. **b** Positive scan (**c**). **d** Relationship between the peak current density and different glucose concentrations at peaks A, B, C, and D

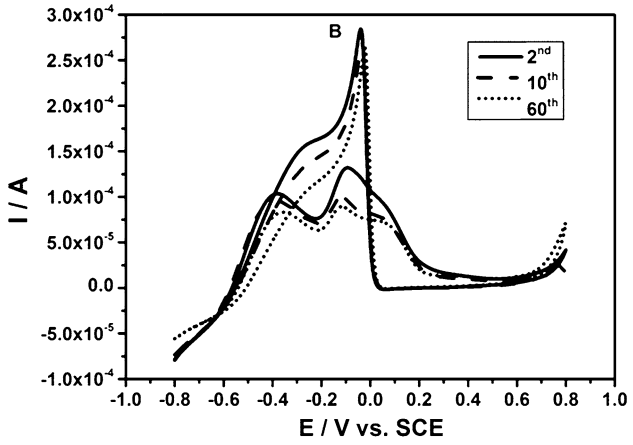

Fig. 9 CV *curves* of the Au NPs/ITO for glucose oxidation (2nd, 10th, and 60th cycle) in 0.5 M KOH with 10 mM glucose at a scan rate of 50 mV/s

than those of previous reports, whereas the amount of auric chloride acid used in our study was much less. Compared with the sensitivity of other glucose sensors based on Au NPs, our voltammetric detection sensitivity was considerably higher [19]. The excellent sensitivity may be attributed to the synergy between PDA and Au NPs. First, the Au NPs decorated ITO has improved specific surface area to accumulate large amount of glucose molecules. Second, π–π stacks in PDA could be used as mediated electron transfer between Au NPs and ITO [20], which accelerated the electron transfer and promoted the process of redox reaction of glucose.

To detect the stability of the Au NPs during the electrocatalytic oxidation of glucose, we recorded CV curves after 2, 10, and 60 potential cycles (Fig. 9). From the 10th to the 60th cycle, the current densities of Au NPs/ITO were maintained from at least 95 to 93 % of their initial values at the characteristic peak B. Therefore, we conclude that the Au NPs/ITO can sustain relative stability during each cycle.

The amperometric responses at the Au NPs/ITO electrode for the successive addition of 1 mM glucose are presented in Fig. 10. The current density was observed to significantly increase with time. The Au NPs/ITO sensor exhibited a linear current response to glucose concentration in the range of 1–10 mM ($R^2 = 0.8735$) at an applied potential of 0.15 V (Fig. 10a inset) and 1–11 mM ($R^2 = 0.9904$) (Fig. 10b inset) at an applied potential of 0.45 V.

Table 1 Comparison of the different glucose sensors, the table is presented with respect to electrode type, sensitivity, linear range and detection limit

Glucose sensors	Sensitivity (μA/mM/cm^2)	Linear range (up to, mM)	Detection limit (μM)	References
Au NPs/ITO-Dip	524	10	6.25	This work
Au Nps/ITO-electrodeposition	23	11	5	[19]
Au NPs/Ti	140	15	14.8	[21]
DA-AuNPs/GOx	334	–	0.1	[22]
Au nanowire array	40	20	3	[23]
Pt–Pb alloy	17.8	11	1.8	[24]

Comparison of the different glucose sensors is shown in Table 1. Our work exhibited a much higher sensitivity compared with other study, though the detection limit 6.25 uM is not the lowest, it is enough for the detection of physiological levels, which is from 3 to 8 mM. Thus, although the EASA of the Au NPs/ITO by dopamine reduction was smaller than those reported by other scholars, the sensitivity and stability rendered the fabricated materials valuable for actual use.

4 Conclusions

The method demonstrated herein produced Au NPs with uniform distribution through a simple, solution-processable step. Our approach employed the SILAR technique by chemically reducing the precursor metal salts with dopamine aqueous solution. Au NPs decorated on the ITO substrate were approximately spherical, with particle sizes

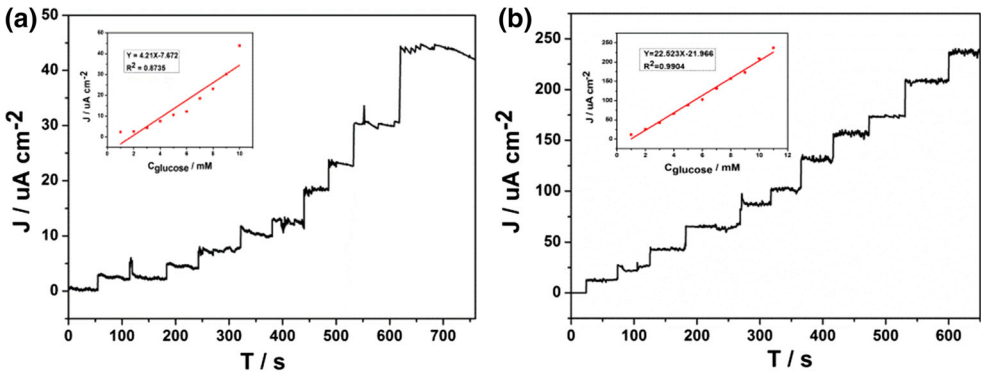

Fig. 10 Chronoamperometric current responses of the Au NPs/ITO electrode. Glucose was injected at regular intervals of about 55 s in the stirred KOH solution at applied potentials of **a** 0.15 and **b** 0.45 V. *Inset* Calibration plot of the concentration of glucose versus current density

that varied in accordance with different SILAR cycles, reactant concentrations, and intermediate media. SERS and absorption spectra confirmed the SPR characteristics of Au. Glucose sensors based on this kind of Au NPs/ITO presented high sensitivity and stability. The detection limit was about 6 uM, and the current densities were maintained to at least 93 % of their initial values after 60 potential cycles. The high sensitivity and stability rendered the fabricated sensors valuable for actual use.

Acknowledgments The work was supported by National Natural Science Foundation of China (11475017).

References

1. D.S. Ginley, C. Bright, Transparent conducting oxide. MRS Bull. **25**, 15 (2000)
2. Y.S. Eng, I. Yasui, D.C. Paine, ITO thin-film transparent conductors: microstructure and processing. Jom-US **47**(3), 47–50 (1995)
3. B.K. Jena, S. Ghosh, R. Bera, R.S. Dey, A.K. Das, C.R. Raj, Bioanalytical applications of au nanoparticles. Recent Pat Nanotechnol **4**(1), 41–52 (2010)
4. J.H.T. Luong, E. Lamb, K.B. Maleb, Recent advances in electrochemical detection of arsenic in drinking and ground waters. Anal. Methods **6**, 6157–6169 (2014)
5. B.-H. Gao, S.-N. Ding, O. Kargbo, Y.-H. Wang, Y.-M. Sun, S. Cosnier, Enhanced electrochemiluminescence of peroxydisulfate by electrodeposited Au nanoparticles and its biosensing application via integrating biocatalytic precipitation using self-assembly bi-enzymes. J. Electroanal. Chem. **703**, 9–13 (2013)
6. Y. Lin, Y. Hu, Y. Long, J. Di, Determination of ascorbic acid using an electrode modified with cysteine self-assembled gold-platinum nanoparticles. Microchim. Acta **175**(3–4), 259–264 (2011)
7. S.H. Chen, C.T. Yen, C.F. Yu, P.C. Kao, C.F. Lin, High PLED enhancement by surface plasmon coupling of Au nanoparticles. Plasmonics **10**(2), 257–261 (2014)
8. D. Zhang, P. Diao, Size-controlled electrochemical synthesis of hemispherical gold nanoparticles on ITO substrates. J. Electroanal. Chem. **755**, 174–181 (2015)
9. X.L. Xu, G.L. Zhou, H.X. Li, Q. Liu, S. Zhang, J.L. Kong, A novel molecularly imprinted sensor for selectively probing imipramine created on ITO electrodes modified by Au nanoparticles. Talanta **78**, 26–32 (2009)
10. L. Yan, K.H. Chan, A. Uddin, Dopamine-induced growth of Au and Ag nanoparticles on ITO substrate and their application in PCPDTBT-based polymer solar cell. Plasmonics (2016). doi:10.1007/s11468-016-0270-x
11. Y. Ma, J. Di, X. Yan et al., Direct electrodeposition of gold nanoparticles on indium tin oxide surface and its application. Biosens. Bioelectron. **24**(5), 1480–1483 (2009)
12. J. Wang, J. Gong, Y. Xiong et al., Shape-dependent electrocatalytic activity of monodispersed gold nanocrystals toward glucose oxidation. Chem. Commun. **47**(24), 6894–6896 (2011)
13. M.L. Mcgashen, K.L. Davis, M.D. Morris, Surface-enhanced Raman scattering of dopamine at polymer-coated silver electrodes. Anal. Chem. **62**, 846–849 (1990)
14. J.H. An, W.A. El-Said, C.H. Yea, T.H. Kim, J.W. Choi, Surface-enhanced Raman scattering of dopamine on self-assembled gold nanoparticles. J. Nanosci. Nanotechnol. **11**, 4424–4429 (2011)
15. M. Kaya, M. Volkan, New approach for the surface enhanced resonance Raman scattering (SERRS) detection of dopamine at picomolar (pM) levels in the presence of ascorbic acid. Anal. Chem. **84**, 7729–7735 (2012)
16. M. Tominaga, T. Shimazoe, M. Nagashima et al., Electrocatalytic oxidation of glucose at gold–silver alloy, silver and gold nanoparticles in an alkaline solution. J. Electroanal. Chem. **590**(1), 37–46 (2006)
17. M. Tominaga, T. Shimazoe, M. Nagashima et al., Electrocatalytic oxidation of glucose at gold nanoparticle -modified carbon electrodes in alkaline and neutral solutions. Electrochem. Commun. **7**(2), 189–193 (2005)
18. L.A. Larew, D.C. Johnson, Concentration dependence of the mechanism of glucose oxidation at gold electrodes in alkaline media. J Electroanal Chem Interfac. **262**(1), 167–182 (1989)
19. J. Wang, *Gold Nanoparticle Arrays Based on Electrodeposition Technology and Their Applications in Surface Enhanced Raman Spectroscopy and Glucose Sensing [D]* (Shanghai Normal University, Shanghai, 2014)
20. Y. Zhang, L. Mi Chu, Y.T. Yang, W. Deng, M. Ma, S. Xiaoli, Q. Xie, Three-dimensional graphene networks as a new substrate for immobilization of laccase and dopamine and its application in glucose/O2 biofuel cell. ACS Appl. Mater. Interfac **6**, 12808–12814 (2014)
21. Q. Yi, W. Yu, Nanoporous gold particles modified titanium electrode for hydrazine oxidation. J. Electroanal. Chem. **633**(1), 159–164 (2009)
22. Y. Wei, *Study on Building, Mechanism and Application of Glucose Biosensor*. Ph.D. Thesis, East China Normal University, China, 2011
23. S. Cherevko, C.H. Chung, Gold nanowire array electrode for non-enzymatic voltammetric and amperometric glucose detection. Sens. Actuator B-Chem **142**(1), 216–223 (2009)
24. Y.W. Lee, N.H. Kim, K.Y. Lee et al., Synthesis and characterization of flower-shaped porous Au-Pd alloy nanoparticles. J. Phys. Chem. C **112**(17), 6717–6722 (2008)